四川大学学报（医学版） 2024，55（2）：290－296
J Sichuan Univ（Med Sci） doi: 10.12182/20240360506

在线全文

颞下经小脑幕入路的显微解剖学研究*

程进超[1,2]，王其福[3,4]，李 陈[4]，荣 军[3,4]，李廷政[1,4]，李 敏[5]，白瑞军[5△]

1. 宣城市中心医院 神经外科（宣城 242000）；2. 南京医科大学鼓楼临床医学院（南京 210000）；
3. 皖南医学院第一附属医院（弋矶山医院）神经外科（芜湖 241000）；4. 皖南医学院神经系统疾病转化医学中心（芜湖 241000）；
5. 无锡市骨科医院（苏州大学附属无锡九院）关节外科（无锡 214000）

【摘要】 目的 研究颞下经小脑幕入路到脑干侧方的显微解剖结构，为脑干侧方、环池、岩斜区域临床手术提供解剖学资料。**方法** 在8例（16侧）发育正常成人尸头标本上进行颞下经小脑幕入路解剖学研究，尸头偏向一侧以颧弓根部为最高点，耳廓上方行马蹄形切口，以颧弓中点为切口前端，后缘达横窦中外侧三分之一处，皮瓣翻向颞部。去除骨瓣后，在显微镜下剔除蛛网膜及软脑膜，观察手术入路的暴露范围，明确途径中相关神经及血管的位置关系，对重要结构进行拍照及测量相关参数。**结果** 颧弓根部上缘可准确定位中颅窝底，10例成年人颅骨标本的星点至乳突尖部、星点至外耳道上脊、顶乳突缝前角至外耳道上脊、顶乳突缝前角至星点的平均距离分别为47.23 mm、45.27 mm、26.16 mm、23.08 mm。颞下入路在切开小脑幕后可充分暴露上至后床突下至岩骨脊、弓状隆起的区域，可以处理中斜坡、环池、中脑和桥脑腹侧面或外侧面的病变，并可通过颧骨切除扩大幕上的显露区域，岩骨磨除技术扩大幕下的显露范围，其中滑车神经全长、距小脑幕缘的距离、在小脑幕夹层中走形长度、穿入幕下处距离岩骨脊的距离分别为（16.95±4.74）mm、（1.27±0.73）mm、（5.72±1.37）mm、（4.51±0.39）mm。 通过后床突或弓状隆起作为定位安全打开小脑幕，动眼神经可作为解剖标志定位大脑后动脉和小脑上动脉。**结论** 通过显微解剖学研究，可明确颞下经小脑幕入路的暴露范围、术中的难点，有利于临床医师精准安全地规划手术方式，降低手术并发症。

【关键词】 颞下入路 小脑幕 中颅窝 滑车神经 显微解剖

Microanatomical Investigation of the Subtemporal Transtentorial Approach *CHENG Jinchao*[1,2], *WANG Qifu*[3,4], *LI Chen*[4], *RONG Jun*[3,4], *LI Tingzheng*[1,4], *LI Min*[5], *BAI Ruijun*[5△]. 1. *Department of Neurosurgery, Xuancheng Central Hospital*, Xuancheng 242000, China; 2. *Gulou School of Clinical Medicine, Nanjing Medical University*, Nanjing 210000, China; 3. *Department of Neurosurgery, The First Affiliated Hospital/Yijishan Hospital of Wannan Medical College*, Wuhu 241000, China; 4. *Translational Research Institute for Neurological Disorders, Wannan Medical College*, Wuhu 241000, China; 5. *Department of Joint Surgery, Wuxi Orthopaedics Hospital/Wuxi 9th People's Hospital Affiliated to Soochow University*, Wuxi 214000, China

△ Corresponding author, E-mail: bairuijuncola0723@suda.edu.cn

【Abstract】 Objective To study the microanatomic structure of the subtemporal transtentorial approach to the lateral side of the brainstem, and to provide anatomical information that will assist clinicians to perform surgeries on the lateral, circumferential, and petroclival regions of the brainstem. **Methods** Anatomical investigations were conducted on 8 cadaveric head specimens (16 sides) using the infratemporal transtentorial approach. The heads were tilted to one side, with the zygomatic arch at its highest point. Then, a horseshoe incision was made above the auricle. The incision extended from the midpoint of the zygomatic arch to one third of the mesolateral length of the transverse sinus, with the flap turned towards the temporal part. After removing the bone, the arachnoid and the soft meninges were carefully stripped under the microscope. The exposure range of the surgical approach was observed and the positional relationships of relevant nerves and blood vessels in the approach were clarified. Important structures were photographed and the relevant parameters were measured. **Results** The upper edge of the zygomatic arch root could be used to accurately locate the base of the middle cranial fossa. The average distances of the star point to the apex of mastoid, the star point to the superior ridge of external auditory canal, the anterior angle of parietomastoid suture to the superior ridge of external auditory canal, and the anterior angle of parietomastoid suture to the star point of the 10 adult skull specimens were 47.23 mm, 45.27 mm, 26.16 mm, and 23.08 mm, respectively. The subtemporal approach could fully expose the area from as high as the posterior clinoid process to as low as the petrous ridge and the arcuate protuberance after cutting through the cerebellar tentorium. The approach makes it possible to handle lesions on the ventral or lateral sides of the middle clivus, the cistern ambiens, the midbrain, midbrain, and pons. In addition, the approach can significantly expand the

* 安徽省临床医学研究转化专项（No. 202204295107020060）资助

△ 通信作者，E-mail: bairuijuncola0723@suda.edu.cn

出版日期：2024-03-20

exposure area of the upper part of the tentorium cerebelli through cheekbone excision and expand the exposure range of the lower part of the tentorium cerebelli through rock bone grinding technology. The total length of the trochlear nerve, distance of the trochlear nerve to the tentorial edge of cerebellum, length of its shape in the tentorial mezzanine, and its lower part of entering into the tentorium cerebelli to the petrosal ridge were (16.95±4.74) mm, (1.27±0.73) mm, (5.72±1.37) mm, and (4.51±0.39) mm, respectively. The cerebellar tentorium could be safely opened through the posterior clinoid process or arcuate protrusion for localization. The oculomotor nerve could serve as an anatomical landmark to locate the posterior cerebral artery and superior cerebellar artery. **Conclusion** Through microanatomic investigation, the exposure range and intraoperative difficulties of the infratemporal transtentorial approach can be clarified, which facilitates clinicians to accurately and safely plan surgical methods and reduce surgical complications.

【Key words】 Subtemporal approach　Tentorium cerebelli　Middle cranial fossa　Trochlear nerve　Microanatomy

脑干在颅脑的中心区域，既是调节和控制人生理活动最重要的高级中枢，也是神经核团和神经纤维走形最密集的地方[1]。脑干发生病变将造成巨大危害[2]。脑干、岩斜区、小脑幕周围分布大量重要的神经及血管，手术操作空间狭小，在手术中损伤神经或血管将给病人带来巨大后遗症甚至死亡[3]。临床手术显露脑干侧方、岩斜区、中颅底的手术入路有多种，其中颞下经小脑幕入路，可以处理中颅窝脑膜瘤、三叉神经鞘瘤、低位的基底动脉动脉瘤是临床医师常用的手术入路[4]。本研究通过尸头标本模拟颞下经小脑幕入路到达中脑、桥脑侧方区域，对其相关解剖学结构进行了逐层研究，为临床医师手术提供解剖学资料。

1　材料与方法

1.1　材料

由皖南医学院神经疾病转化医学中心解剖学教研室提供10例发育正常的成年人颅骨，8例成年中国人尸头标本。经福尔马林溶液充分固定，8例尸头标本的性别、年龄不详。分离出相关动静脉，在动脉、静脉分别注入按比例配好的红色和蓝色硅胶溶液。本研究获得宣城市中心医院伦理委员会批准（审批号No.2024004），器械和仪器由皖南医学院神经疾病转化医学实验室提供包括：尸头标本架、神经外科显微器械、史赛克高速磨钻、莱卡手术显微镜（M320F12）、游标卡尺、圆规、尼康（JY670）单反相机等。

1.2　方法

将标本放置于标本架上，尸头偏向一侧以颧弓根部为最高点，耳廓上方行马蹄形切口，以颧弓中点为切口前端，后缘达横窦中外侧三分之一处，皮瓣翻向颞部（图1）。去除骨瓣后，在显微镜下剔除蛛网膜及软脑膜，手术入路完成后去除遮挡组织暴露重要的血管及神经以便拍照观察。对解剖过程中所有重要结构予以测量数据和记录。

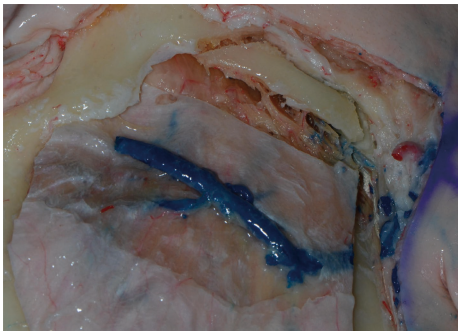

图 1　手术入路操作示意图：去除皮瓣，颞肌层面

Fig 1　Schematic diagram of the surgical approach: removal of the flap and temporalis muscle layer

1.3　统计学方法

应用SPSS 26.0软件对数据进行描述性分析。计量资料以$\bar{x} \pm s$表示，计数资料以率（%）表示。

2　结果

2.1　颞下入路骨性解剖结构

颞骨的解剖结构比较复杂，其和顶骨、枕骨及蝶骨紧密相连，又分为岩部、鳞部、鼓部、乳突和茎突。颞下入路前方需显露达到颧弓根部，后缘达顶乳缝和鳞状缝交点，即横窦和乙状窦前缘。鳞状缝可作为侧裂的颅骨对应标记；乳突上脊位于中颅窝底水平，其和鳞状缝的汇合点位于岩骨脊外侧端。颞骨岩部上表面前方凹陷为三叉神经压迹，其上为Meckels腔，外侧为覆盖于上半规管的弓状隆起。弓状隆起是颞部手术的重要解剖学骨性标志。颞骨外侧面重要骨性解剖标志星点、外耳道上脊，乳突上脊、乳突尖部的相互位置距离和位置关系见表1和图2。

2.2　颞下入路中相关神经解剖结构

经颞下入路，抬起颞叶，打开环池，可在显微镜下直视中颅窝底及小脑幕区域结构（图3~图6）。中脑和桥脑上部在小脑幕内侧，测量得出颧弓后跟至脑干腹侧中线距离为（58.27±6.12）mm。滑车神经是唯一从脑干背侧

表 1 颞部外侧面骨性结构的距离（*n*=10）

Table 1 The distance of lateral temporal bony structure (*n*=10)

Structure	Mean value/mm	Measurement value range/mm
Star point to apex of mastoid	47.23	40.79-59.41
Star point to superior ridge of meatus externa	45.27	43.41-50.28
Anterior angle of parietomastoid suture to superior ridge of external auditory meatus	26.16	20.02-30.21
Anterior angle of parietomastoid suture to star point	23.08	16.12-25.69

图 2 颅骨左侧图

Fig 2 Left side of the skull

1, Zygomatic arch; 2, sphenosquamous suturae; 3, squamous suture; 4, mastoid process, temporal bone; 5, zygomatic bone; 6, external acoustic pore; 7, styloid process of the temporal bone.

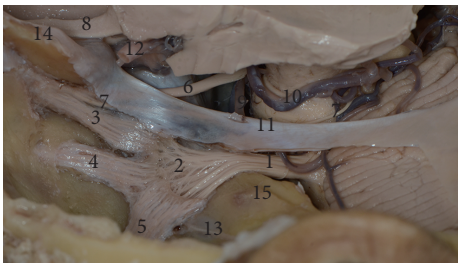

图 3 左侧颅底上面观

Fig 3 The top view of the left skull base

1, Trigeminal nerve; 2, trigeminal ganglion; 3, ophthalmic nerve; 4, maxillary nerve; 5, mandibular nerve; 6, oculomotor nerve; 7, trochlea nerve; 8, optic nerve; 9, superior cerebellar artery; 10, posterior cerebral artery; 11, tentorium cerebelli; 12, internal carotid artery; 13, greater petrosal nerve; 14, anterior clinoid process; 15, arcuate eminence.

发出的颅神经，测量其全长为（16.95±4.74）mm，其绕中脑而行，由小脑幕上方穿行至小脑幕下方。本次研究发现，滑车神经穿行过程中紧贴小脑幕缘，测量滑车神经距小脑幕缘的距离为（1.27±0.73）mm，滑车神经在小脑幕夹层中走形（5.72±1.37）mm再进入海绵窦外侧壁，滑车神经穿入幕下处距离岩骨脊（4.51±0.39）mm。本研究测量得到滑车神经在动眼神经三角后部距离动眼神经（5.12±0.46）mm。动眼神经自脚间窝发出，穿行于大脑后动脉和小脑上动脉之间，经过后床突入海绵窦最后穿入眶上裂；测量动眼神经脑池段全长为（9.97±2.81）mm。三叉

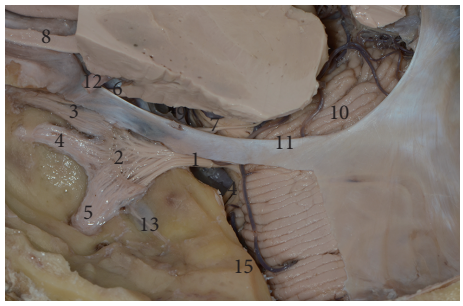

图 4 左侧中颅底侧后方图

Fig 4 The Lateral posterior view of the left middle skull base

1, Trigeminal nerve; 2, trigeminal ganglion; 3, ophthalmic nerve; 4, maxillary nerve; 5, mandibular nerve; 6, oculomotor nerve; 7, trochlea nerve; 8, optic nerve; 9, superior cerebellar artery; 10, cerebellum; 11, tentorium cerebelli; 12, internal carotid artery; 13, greater petrosal nerve; 14, facial nerve; 15, arcuate eminence.

图 5 左侧中颅窝底解剖图

Fig 5 The anatomical diagram of base upon the left middle fossa

1, Trigeminal ganglion; 2, ophthalmic nerve; 3, maxillary nerve; 4, mandibular nerve; 5, greater petrosal nerve; 6, trochlea nerve; 7, oculomotor nerve; 8, optic nerve; 9, olfactory nerve; 10, internal carotid artery; 11, anterior cerebral artery; 12, internal carotid artery petrosal segment; 13, posterior cerebral artery; 14, superior cerebellar artery; 15, arcuate eminence.

神经起自桥脑中部，周边血管丰富，小脑上动脉、小脑前下动脉及岩静脉均有可能压迫神经。测量三叉神经和滑车神经的距离为（5.36±0.75）mm，三叉神经后跟到小脑幕缘的距离为（1.02±0.14）mm。

2.3 颞下入路的血管解剖结构

见图7~图10。Labble静脉是跨越颞叶外侧、连接外侧裂及横窦之间最大的吻合静脉。我们观测到其起自外侧裂中部，汇入横窦前部。总共8例标本16根Labble静脉

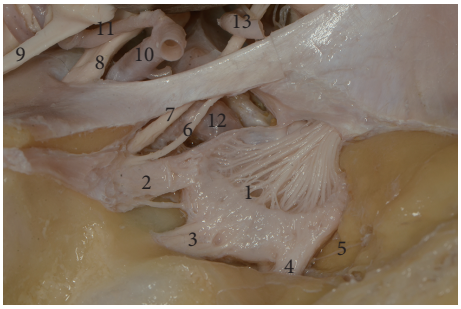

图 6 左侧中颅窝颅底解剖图

Fig 6 The anatomy of skull base upon the left middle cranial fossa

1, Trigeminal ganglion; 2, ophthalmic nerve; 3, maxillary nerve; 4, mandibular nerve; 5, greater petrosal nerve; 6, trochlea nerve; 7, oculomotor nerve; 8, optic nerve; 9, olfactory nerve; 10, internal carotid artery; 11, anterior cerebral artery; 12, internal carotid artery petrosal segment; 13, posterior cerebral artery.

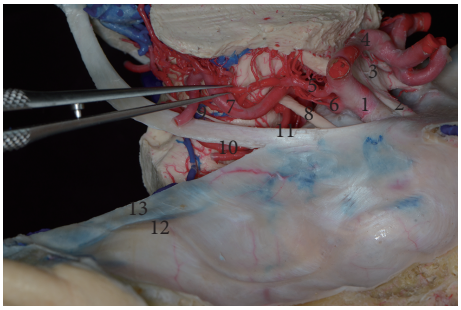

图 7 右侧颅底灌注标本图

Fig 7 Right skull base perfusion specimen

1, Internal carotid artery; 2, optic nerve; 3, optic chiasma; 4, anterior cerebral artery; 5, anterior choroidal artery; 6, posterior communicating artery; 7, posterior cerebral artery; 8, oculomotor nerve; 9, trochlea nerve; 10, superior cerebellar artery; 11, tentorium cerebelli; 12, arcuate eminence; 13, superior petrosal sinus.

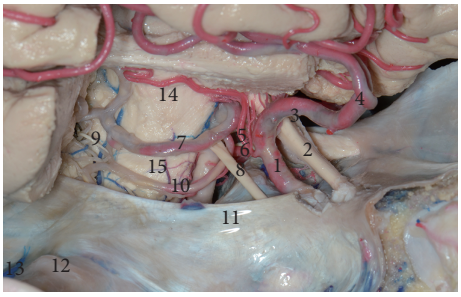

图 8 右侧中颅底灌注标本解剖图

Fig 8 The anatomy of right middle skull base perfusion specimen

1, Internal carotid artery; 2, optic nerve; 3, optic chiasma; 4, anterior cerebral artery; 5, anterior choroidal artery; 6, posterior communicating artery; 7, posterior cerebral artery; 8, oculomotor nerve; 9, trochlear nerve; 10, superior cerebellar artery; 11, tentorium; 12, arcuate eminence; 13, superior petrosal sinus; 14, mesencephalon; 15, pons.

中, 2根位于颞叶的前1/3, 占比12.5%; 10根位于颞叶中部靠后处, 占比62.5%; 4根位于颞叶后界, 占比25.0%。所有Labble静脉全部注入横窦未见缺如。

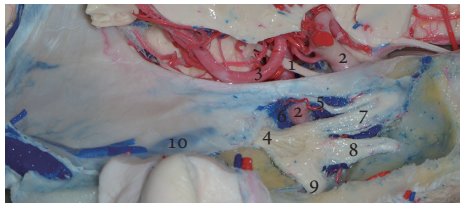

图 9 右侧中颅底灌注标本侧方图

Fig 9 The lateral view of right middle skull base perfusion specimen

1, Oculomotor nerve; 2, internal carotid artery; 3, posterior cerebral artery; 4, trigeminal nerve; 5, trochlear nerve; 6, cavernous sinus; 7, ophthalmic nerve; 8, maxillary nerve; 9, mandibular nerve; 10, sinuses petrosus superior.

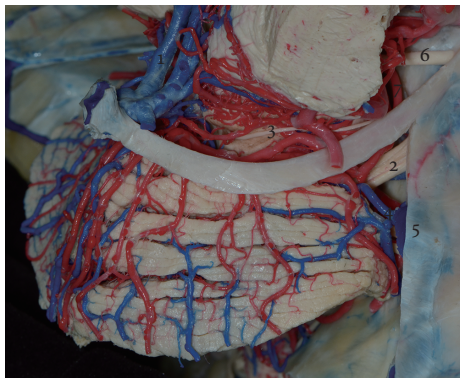

图 10 小脑侧后方灌注标本图

Fig 10 Posterior perfusion specimen of cerebellar side

1, Great cerebral vein; 2, trigeminal nerve; 3, trochlear nerve; 4, petrosa vein; 5, sinuses petrosus superior; 6, oculomotor nerve; 7, superior cerebellar artery.

环池内、小脑幕、中脑及桥脑区域血管复杂, 后床突和动眼神经是最为容易观察到的解剖结构, 后床突作为骨性结构位置较为恒定, 因此本研究测量了重要的血管和神经结构距离后床突的距离(表2)。观察到动眼神经后即可找到位于动眼神经上方的大脑后动脉和下方的小脑上动脉, 并可沿大脑后动脉发现后交通动脉。大脑后动脉距离小脑幕缘的距离为(3.29±0.51) mm, 大脑后动脉起自基底动脉分叉部, 可在脚间池外侧缘发现后交通动脉。测量大脑后动脉P2段长度为(49.39±5.86) mm, 大脑后动脉P2段可发出大脑脚穿动脉。本研究8例标本共16侧, 测得数据为发出2支大脑脚穿动脉为6侧, 占比37.5%; 发出3支的为7侧, 占比43.75%; 发出4支的为3侧,

表 2 后床突到各结构位置的距离 (*n*=16)

Table 2 Distance of rear bed process to each structural position (*n*=16)

Structure	Mean value/mm	Measurement value range/mm
The trochlear nerve penetrating the entrance to the tentorium	15.36	12.48-17.76
Posterior cerebral artery	4.35	3.23-6.71
Superior cerebellar artery	5.71	3.42-7.97
Posterior communicating artery	3.17	2.31-5.18

占比18.75%。大脑脚穿动脉主要供应皮质脊髓束、皮质核束及黑质红核,大脑后动脉大部位于幕上,小脑上动脉大部位于幕下,幕上的长度短,切开小脑幕可增加小脑上动脉的暴露。

岩上静脉注入岩上窦,我们发现16个岩上窦中,1个有3支岩上静脉,占比6.25%;6个有两支岩上静脉,占比37.5%;9个有1支岩上静脉,占比56.25%。总共测得24支岩上静脉。我们根据其和注入岩上窦的位置关系,分为内侧、中间、外侧三组。15支为内侧型,占比62.5%;2支为中间型,占比8.3%;7支为外侧型,占比29.2%。

3 讨论

颞下入路是神经外科医师的常用手术入路。可以较清晰地从侧方暴露脑干、环池[5]。其中桥脑上部解剖显露范围上方至小脑上动脉,下方至三叉神经内侧;中脑侧方可暴露范围是上至脉络膜前动脉,下至大脑后动脉[6],具有垂直视角大,操作距离短,暴露范围广的优点。

颞下入路在释放脑脊液后,上抬颞叶时必须要注意对Labble静脉的保护。Labble静脉是颞前、颞中、颞外侧静脉的引流静脉,一旦损伤或牵拉过度则会引起术后脑水肿、癫痫、失语等一系列严重并发症[7-8]。本研究发现因下吻合静脉的解剖位置关系会导致颞叶尤其是颞叶后部上抬受限,从而影响颞下入路的手术显露。所以术前对患者行MRV、CTV等相关检查对Labble静脉走行及回流横窦解剖位置的评估十分重要,将决定术中的视野暴露效果。有研究认为汇入横窦但距离静脉窦角小于1 cm和直接汇入岩上窦的Labble静脉称为Labble静脉前置,会严重影响颞叶的上抬,应避免使用颞下入路[9-10]。颞下入路手术中,如何无损伤地切开小脑幕是手术的重点及难点,所以小脑幕切迹及其周围血管和滑车神经的解剖位置关系十分重要[11]。小脑幕为双层硬脑膜结构,内侧为小脑幕游离缘,前方附着于岩尖和前、后床突,后缘达枕骨横窦沟内。手术中切开小脑幕缘,要十分注意避免损伤滑车神经,其和小脑幕缘关系十分密切。滑车神经起自脑干背侧、中脑下丘下方,沿脑干外侧环形接近岩骨脊处入小脑幕缘,并在小脑幕夹层中走形后进入海绵窦外侧壁。部分学者认为可通过动眼神经到滑车神经进入小脑幕缘入口处的距离或动眼神经到大脑后动脉的交点同小脑幕的垂线来确定剪开小脑幕缘的位置[12]。但该方案不仅解剖数据变异较大,且实际临床手术中病变易对大脑后动脉和动眼神经产生挤压,使其偏离原来位置,影响手术安全。笔者认为应当更多采用固定位置或骨性解剖位置来确定滑车神经进入小脑幕缘的位置。骨性解剖标志相对较为恒定,可在滑车神经进入小脑幕后方1 cm处可安全切开小脑幕,并可用岩上窦或弓状隆起作为骨性解剖标志。陈永汉等[13]认为可以后床突为标记点,在后床突外后方1.8 cm处安全切开小脑幕缘,和本实验所得数据相同。切开小脑幕后,手术视野可进一步扩展,可暴露海绵窦外侧、视交叉后部到小脑幕中切迹、上岩斜区、中后颅窝及部分桥小脑角区。且颞下经小脑幕入路处理中颅窝病变相较于颞下-岩前入路无需磨除岩骨,创伤更小,风险更低[14]。

部分学者在颞下入路术中仅仅重视对大脑后动脉、小脑上动脉的保护,而忽略了岩静脉的重要性。依据岩静脉注入岩上窦的位置可将其分为外侧、中间、内侧三组。岩静脉损伤,导致回流受阻可导致小脑功能障碍、听觉功能障碍[15]。术中应保护岩静脉的完整性,如果必须结扎岩上窦,则需要在距离三叉神经Meckel腔侧1 cm内,岩静脉入岩上窦内侧结扎离断[16]。

到达脑干侧方、环池、岩斜区、中颅底的手术入路有多种。本研究还发现颞下入路可通过经脑沟提供到达海马区域病灶的通道,通过经皮质-脑室-经脉络膜入路可达到基底池。通过这一入路可对诸如颅中窝脑膜瘤、小型听神经瘤、三叉神经鞘瘤、低位的基底动脉顶端和上方动脉瘤、上岩斜区脑膜瘤进行有效暴露[17-19]。颞下入路灵活多变可与扩大翼点入路相结合,用于暴露脚间池的复杂血管畸形以及扩展到小脑幕裂孔和视交叉旁区的多间隔脑膜瘤[20-21]。但因为受到Labble静脉影响颞叶上抬高度受限,颞下入路对后交通动脉之上的中脑病变,基底动脉分叉部之上的动脉瘤暴露不足[22]。为了减少对颞叶牵拉的影响,增加手术视野暴露,RHOTON[23]认为颧弓根部上缘可准确定位中颅窝底,开颅中应尽可能咬平骨窗,平中颅窝底,移除颧弓上缘可增加手术暴露。也有部分学者认为抬起颞叶时尚不能到达基底池释放脑脊液,可通过术前行腰大池置管引流来减轻对颞叶的牵拉。颞下入路同经典的翼点入路在小脑幕缘前部、前床突和鞍区暴露范围接近,但在后床突、鞍背及小脑幕中切迹区域颞下入路优势明显,反之翼点入路在对侧裂区域的暴露优于颞下入路[6]。颞下入路和其他经典手术入路进行联合,降低患者并发症增加手术效果,也将是未来研究方向。

综上所述,本研究发现颞下入路在切开小脑幕后可充分暴露上至后床突下至岩骨脊、弓状隆起的区域。可以处理中斜坡、环池、中脑和桥脑腹侧面或外侧面的病变。并可通过颧骨切除显著扩大幕上的显露区域,岩骨磨除技术扩大幕下的显露范围。颞下入路相关区域解剖复杂,手术难度较高,术前应完善影像学及血管成像检

查, 明确Labble静脉对手术的影响, 选择合适的手术入路。且神经外科手术医师经过颅底解剖培训, 熟知有关解剖学知识, 对手术的安全性有十分积极的意义。

*　　*　　*

作者贡献声明　程进超负责论文构思、数据审编、正式分析和研究方法, 王其福负责数据审编和调查研究, 李陈负责调查研究, 荣军负责正式分析, 李廷政负责可视化, 李敏负责调查研究, 白瑞军负责研究方法、研究项目管理和审读与编辑写作。所有作者已经同意将文章提交给本刊, 且对将要发表的版本进行最终定稿, 并同意对工作的所有方面负责。

Author Contribution　CHENG Jinchao is responsible for conceptualization, data curation, formal analysis, and methodology. WANG Qifu is responsible for data curation and investigation. LI Chen is responsible for investigation. RONG Jun is responsible for formal analysis. LI Tingzheng is responsible for visualization. LI Min is responsible for investigation. BAI Ruijun is responsible for methodology, project administration, and writing--review and editing. All authors consented to the submission of the article to the Journal. All authors approved the final version to be published and agreed to take responsibility for all aspects of the work.

利益冲突　所有作者均声明不存在利益冲突

Declaration of Conflicting Interests　All authors declare no competing interests.

参 考 文 献

[1] RUDER L, SCHINA R, KANODIA H, *et al*. A functional map for diverse forelimb actions within brainstem circuitry. Nature, 2021, 590(7846): 445–450. doi: 10.1038/s41586-020-03080-z.

[2] ABLA A A, LEKOVIC G P, GARRETT M, *et al*. Cavernous malformations of the brainstem presenting in childhood: surgical experience in 40 patients. Neurosurgery, 2010, 67(6): 1589–1598. doi: 10.1227/NEU.0b013e3181f8d1b2.

[3] SCHACKERT G, LENK M, KIRSCH M, *et al*. Surgical results of 158 petroclival meningiomas with special focus on standard craniotomies. J Neurooncol, 2022, 160(1): 55–65. doi: 10.1007/s11060-022-04105-5.

[4] XU Z, WANG W, ZHANG J, *et al*. Subtemporal-anterior transtentoral approach to middle cranial fossa microsurgical anatomy. J Craniofac Surg, 2014, 25(6): 2220–2222. doi: 10.1097/scs.0000000000001073.

[5] CAVALCANTI D D, MORAIS B A, FIGUEIREDO E G, *et al*. Accessing the anterior mesencephalic zone: orbitozygomatic versus subtemporal approach. World Neurosurg, 2018, 119: e818–e824. doi: 10.1016/j.wneu.2018.07.272.

[6] TANG Y, WANG H D, MA C Y, *et al*. Quantitative anatomic comparison of the extended pterional transtemporal transtentorial approach and the subtemporal transtentorial approach to the petroclival region. Turk Neurosurg, 2015, 25(1): 9–15. doi: 10.5137/1019-5149.Jtn.7450-13.1.

[7] 刘庆良, 王忠诚, 张俊廷. 颞枕入路Labbe静脉术中结扎术后失语分析. 中华神经外科杂志, 1997, 13(2): 34–36. doi: 10.3760/j.issn:1001-2346.1997.02.015.
LIU Q L, WANG Z C, ZHANG J T. Analysis of speech with the Labbe vein ligated in tempoccipital operation. Chin J Neurosurg, 1997, 13(2): 34–36. doi: 10.3760/j.issn:1001-2346.1997.02.015.

[8] CANDANEDO C, MOSCOVICI S, SPEKTOR S. The infratranstentorial subtemporal approach (ITSTA): a valuable skull base approach to deep-seated non-skull base pathology. Acta Neurochir (Wien), 2019, 161(11): 2335–2342. doi: 10.1007/s00701-019-04050-9.

[9] 王轩, 佟小光. 联合经岩入路手术中相关静脉结构及硬膜的处理策略. 中华神经外科杂志, 2023, 39(12): 1189–1194. doi: 10.3760/cma.j.cn112050-20230311-00071.
WANG X, TONG X G. Combined with the management strategy of related venous structures and dura mater in the transpetrosal approach. Chin J Neurosurg, 2023, 39(12): 1189–1194. doi: 10.3760/cma.j.cn112050-20230311-00071.

[10] GARCÍA-PÉREZ D, ABARCA J, GONZÁLEZ-LÓPEZ P, *et al*. A frontal route to middle and posterior cranial fossa: quantitative study for the lateral transorbital endoscopic approach and comparison with the subtemporal approach. World Neurosurg, 2022, 167: e236–e250. doi: 10.1016/j.wneu.2022.07.129.

[11] JOO W, RHOTON A L, Jr. Microsurgical anatomy of the trochlear nerve. Clin Anat, 2015, 28(7): 857–864. doi: 10.1002/ca.22602.

[12] 李学民, 书国伟, 王勇. 颞下经小脑幕入路至上岩斜区应用解剖研究. 中国临床神经外科杂志, 2009, 14(4): 219–221. doi: 10.13798/j.issn.1009-153x.2009.04.003.
LI X M, SHU G W, WANG Y. Study of applied anatomy related to neurosurgery through subtemporal transtentorial approach to superior petroclival region. Chin J Clin Neurosurg, 2009, 14(4): 219–221. doi: 10.13798/j.issn.1009-153x.2009.04.003.

[13] 陈永汉, 白锡波, 田耀辉, 等. 经颞下入路对基底动脉顶端区域显微解剖研究. 脑与神经疾病杂志, 2013, 21(2): 145–148. doi: 10.3969/j.issn.1006-351X.2013.02.021.
CHEN Y H, BAI X B, TIAN Y H, *et al*. The microsurgical anatomy study of basilar artery apex via subtcmporal approach. J Brain Ner Dis, 2013, 21(2): 145–148. doi: 10.3969/j.issn.1006-351X.2013.02.021.

[14] KIM S M, PAEK S H, LEE J H. Infratemporal fossa approach: the modified zygomatico-transmandibular approach. Maxillofac Plast Reconstr Surg, 2019, 41(1): 3. doi: 10.1186/s40902-018-0185-x.

[15] KIM M, PARK S K, LEE S, *et al*. Prevention of superior petrosal vein injury during microvascular decompression for trigeminal neuralgia: operative nuances. J Neurol Surg B Skull Base, 2022, 83(Suppl 2): e284–e290. doi: 10.1055/s-0041-1725036.

[16] YOKOSAKO S, KIKUCHI A, OHBUCHI H, *et al*. Venous flow conversion technique for sacrificing the superior petrosal vein during microvascular decompression for trigeminal neuralgia. Oper Neurosurg (Hagerstown), 2022, 23(4): e232–e236. doi: 10.1227/ons.0000000000000333.

[17] KELEŞ A, ARMSTRONG S A, SAYYAHMELLI S, *et al*. Microsurgical resection of a large petroclival meningioma via translabyrinthine

approach combined with middle fossa craniotomy. Neurosurg Focus Video, 2022, 6(2): V11. doi: 10.3171/2022.1.Focvid21253.

[18] OGIWARA T, GOTO T, KUSANO Y, *et al*. Subtemporal transtentorial approach for recurrent trigeminal neuralgia after microvascular decompression via the lateral suboccipital approach: case report. J Neurosurg, 2015, 122(6): 1429–1432. doi: 10.3171/2014.10.Jns132643.

[19] Von RHEIN B, NELLES M, URBACh H, *et al*. Neuropsychological outcome after selective amygdalohippocampectomy: subtemporal versus transsylvian approach. J Neurol Neurosurg Psychiatry, 2012, 83(9): 887–893. doi: 10.1136/jnnp-2011-302025.

[20] LAMKI T, SALMA A, BAIDYA N, *et al*. Path to the interpeduncular fossa: anatomical comparison of endoscopic-assisted versus standard subtemporal approach. J Neurol Surg B Skull Base, 2012, 73(4): 261–264. doi: 10.1055/s-0032-1312717.

[21] SANCHEZ CORREA T E, CEJA D G, MENDEZ-ROSITO D. Subtemporal approach for the resection of a midbrain cavernous malformation: evaluation of safe surgical corridors. Neurosurg Focus Video, 2019, 1(1): V1. doi: 10.3171/2019.7.FocusVid.19135.

[22] LANZINO G, CANNIZZARO D, VILLA S L. Subtemporal approach for distal basilar occlusion for giant aneurysm. Nuances and advantages of the subtemporal approach. Neurosurg Focus, 2015, 38(Video Suppl1): Video5. doi: 10.3171/2015.V1.Focus14536.

[23] RHOTON A L. The temporal bone and transtemporal approaches. Neurosurgery, 2000, 47(3): S211–S265. doi: 10.1097/00006123-200009001-00023.

（2023 – 11 – 30收稿, 2024 – 03 – 08修回）

编辑 汤 洁